Journal of Medicinal Chemistry

Article

pubs.acs.org/jmc

Development of New Cathepsin B Inhibitors: Combining Bioisosteric Replacements and Structure-Based Design To Explore the Structure–Activity Relationships of Nitroxoline Derivatives

Izidor Sosič,[†,⊥] Bojana Mirković,[†,⊥] Katharina Arenz,[†] Bogdan Štefane,[‡,§] Janko Kos,[†,∥] and Stanislav Gobec*[,†]

[†]Faculty of Pharmacy, University of Ljubljana, Aškerčeva 7, 1000 Ljubljana, Slovenia

[‡]Faculty of Chemistry and Chemical Technology, University of Ljubljana, Aškerčeva 5, 1000 Ljubljana, Slovenia

[§]EN-FIST Centre of Excellence, Dunajska 156, 1000 Ljubljana, Slovenia

[∥]Department of Biotechnology, Jožef Stefan Institute, Jamova 39, 1000 Ljubljana, Slovenia

Supporting Information

ABSTRACT: Human cathepsin B has many house-keeping functions, such as protein turnover in lysosomes. However, dysregulation of its activity is associated with numerous diseases, including cancers. We present here the structure-based design and synthesis of new cathepsin B inhibitors using the cocrystal structure of 5-nitro-8-hydroxyquinoline in the cathepsin B active site. A focused library of over 50 compounds was prepared by modifying positions 5, 7, and 8 of the parent compound nitroxoline. The kinetic parameters and modes of inhibition were characterized, and the selectivities of the most promising inhibitors were determined. The best performing inhibitor **17** was effective in cell-based in vitro models of tumor invasion, where it significantly abrogated invasion of MCF-10A neoT cells. These data show that we have successfully explored the structure–activity relationships of nitroxoline derivatives to provide new inhibitors that could eventually lead to compounds with clinical usefulness against the deleterious effects of cathepsin B in cancer progression.

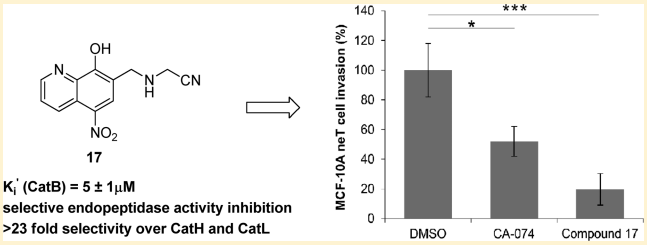

1. INTRODUCTION

Human cathepsin B (catB, EC 3.4.22.1) is a lysosomal cysteine protease that belongs to the papain family (C1) of the CA clan of cysteine proteases.[1] CatB is ubiquitously expressed in a variety of tissues, where it is involved in a number of physiological processes, such as protein turnover in lysosomes,[2] bone remodeling,[3] liberation of thyroid hormones,[4] and antigen processing.[5] However, a number of studies have shown that alterations in catB expression, protein levels, activity, and localization are associated with a variety of diseases, such as Alzheimer's disease,[6] rheumatoid arthritis,[7] osteoarthritis,[8] pancreatitis,[9] and cancers.[10] Of note, elevated catB activity has been shown for many human tumors and has been proposed as a prognostic marker in patients with melanoma and with head and neck, brain, breast, ovarian, colorectal, and lung cancer.[11,12] CatB is localized to perinuclear vesicles in normal cells; however, it has been shown that in transformed and cancer cells, it adopts a more peripheral distribution in the cytoplasm and is associated with the plasma membrane.[13] It can also be secreted into the extracellular environment.[14−16] Once secreted, catB can affect the extracellular matrix (ECM) either directly via proteolytic degradation of its components (collagen type IV, laminin, fibronectin)[17−19] or indirectly via activation or amplification of other proteases in the proteolytic cascade (pro-urokinase plasminogen activator, matrix metalloproteinases 1–3). Both of these events lead to ECM breakdown, a crucial step that enables tumor invasion and metastasis.[16,20]

CatB is unique among the cysteine cathepsins because of its ability to act as both an endopeptidase and a dipeptidyl carboxypeptidase, through removal of dipeptides from the C-terminal of peptidyl substrates.[2] This dual character is attributed to the presence of a ∼20 amino acid insertion, termed the occluding loop.[21] Two salt bridges that attach the loop to the body of the enzyme (Asp22–His110, Asp224–Arg116) limit the access of extended substrates to the primed sites of the active-site cleft, which renders catB a weaker endopeptidase compared to the other cysteine cathepsins.[22,23] Additionally, two histidine residues located at the tip of the occluding loop (His110, His111) provide positively charged anchors for the C-terminal carboxylate group of peptidyl substrates, and this explains the well-known carboxypeptidase activity of catB. This carboxypeptidase activity has a pH optimum of around 5,[24] which associates the exopeptidase activity of catB with its physiological role in the lysosomal compartments. However, the endopeptidase function of catB

Received: October 22, 2012
Published: December 20, 2012

   dx.doi.org/10.1021/jm301544x | J. Med. Chem. 2013, 56, 521−533

greatly increases when the contacts that bind the loop to the body of the enzyme are weakened.[22] This endopeptidase conformation of catB can be stabilized by inhibitors, such as cystatin C,[25] stefin A,[26] and chagasin.[27] Moreover, it has been shown that catB endopeptidase activity increases with increased pH,[24] which indicates that this activity has a vital role in the pathological processes of catB in extralysosomal and extracellular environments (e.g., in degradation of the ECM).

Most of the synthetic catB inhibitors that have been described to date are peptidyl compounds that contain an electrophilic functionality that forms an irreversible or reversible covalent bond with the catalytic cysteine in the active site of catB.[28] Because of their peptidyl nature and reactivity toward off-target proteins, these inhibitors usually have low bioavailability and side effects, which limits them to research use only.[29] Therefore, there is a great need for the discovery of new catB-inhibiting scaffolds that can circumvent the current limitations of these catB inhibitors. Recent studies have focused on the discovery of reversible covalent cysteine cathepsin inhibitors that have a mildly electrophilic "warhead", of which the nitrile-containing functionalities are receiving the most attention mainly because of their reversible mode of inhibition and their low reactivities toward other cellular nucleophiles.[30]

Recently, we described the established antimicrobial agent 5-nitro-8-hydroxyquinoline (nitroxoline, Figure 1) as a potent,

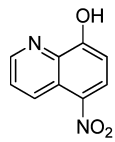

Nitroxoline

Endopeptidase activity
K_i (μM) = 154.4 ± 26.7, K_i' (μM) = 39.5 ± 2.8
mixed inhibition

Exopeptidase activity
K_i (μM) = 271.8 ± 11.2
noncompetitive inhibition

Figure 1. Nitroxoline (5-nitro-8-hydroxyquinoline) and its endopeptidase and exopeptidase inhibition of catB.[31]

selective, and reversible inhibitor of catB endopeptidase activity.[31] Moreover, we reported the cocrystal structure of nitroxoline in the active site of catB (PDB code 3AI8), and as evident from this structure, the nitro group of nitroxoline interacts with two histidines in the occluding loop of catB (His110 and His111). This is in agreement with previous studies that have reported selective catB inhibition through interactions with the occluding loop, a unique feature of catB.[32,33] However, the cocrystal structure also indicated that this inhibition can still be improved upon by modifying the structure of nitroxoline to fill the empty S1′ pocket and by introducing an electrophilic "warhead" that can form reversible covalent interactions with the active site thiol. Therefore, we report here the design and synthesis of a focused library of compounds that were used to explore the structure–activity relationships of nitroxoline derivatives against catB endopeptidase and exopeptidase activities. Our efforts have resulted in the synthesis of a novel, selective, and potent catB inhibitor, compound **17**, which primarily inhibits catB endopeptidase activity and impairs this enzyme activity in cell-based in vitro models of tumor invasion.

2. DESIGN

The crystal structure of nitroxoline[31] in the catB active site was used as the starting point for further derivatization and optimization to find new catB inhibitors. From the druglikeness point of view, the 5-nitro-8-hydroxy scaffold of nitroxoline offers many opportunities for optimization, as it is a very small molecule and it can be readily modified synthetically. To establish the structure–activity relationships of the synthesized compounds, we pursued four different approaches (Figure 2).

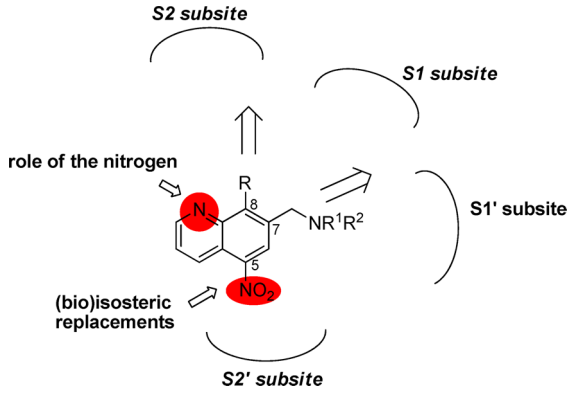

Figure 2. Schematic representation of the modifications to nitroxoline.

First, we evaluated whether the NO_2 group can be replaced with its (bio)isosteres. Next, we synthesized several derivatives with different substitutions at position 7 of nitroxoline. Third, we synthesized a variety of 8-substituted 5-nitroquinolines, and finally, we replaced the quinoline ring with a naphthalene moiety on a limited number of compounds to determine the role of the bicyclic aromatic system in catB inhibition.

3. CHEMISTRY

3.1. Synthesis of the Nitro Group (Bio)Isosteres. Compounds **1**–**6** were synthesized under the conditions of Skraup synthesis (Scheme 1). Variously substituted 2-hydroxyanilines were mixed with acrolein (or crotonaldehyde in the case of compound **6**) in the presence of 6 M HCl at 100 °C for 1 h. Although the yields were moderate, this procedure allowed us to obtain compounds with most of the recently described NO_2 group isosteres (COOH, compounds **1**, **5**, and **6**; SO_3H, compound **2**; SO_2CH_3, compound **3**; CF_3, compound **4**).[34] Moreover, the carboxyl groups of compounds **5** and **6** were converted into methyl esters (compounds **7** and **8**), as this moiety was also described as a NO_2 group bioisostere. For the esterification, we used diazomethane that was freshly prepared before the reaction. However, under the reaction conditions applied, there was concurrent methylation of the hydroxyl group of the ring in both cases (Scheme 1). To accurately cover the majority of the alternative NO_2 substituents described in the literature,[34] we additionally purchased two compounds, namely, 5-fluoro-8-hydroxyquinoline (**9**) and 4-hydroxy-1,5-naphthyridine (**10**), the latter with the pyridine nitrogen as an aromatic NO_2 group isostere (Table S1, Supporting Information).

3.2. Modifications to Position 7 of Nitroxoline. The 7-substituted nitroxoline derivatives were obtained via previously described procedures.[35] By applying the Mannich reaction conditions, we synthesized several structurally diverse 7-aminomethylated derivatives **11**–**20** in good yields (Scheme 2, Table 1). Compound **21** was obtained from **20** using alkaline hydrolysis. Additionally, we synthesized two compounds with small and relatively polar substituents at position 7 of the quinoline ring: compound **23** was obtained by nitration of 8-hydroxyquinoline (**22**), whereas compound **25** was obtained by

dx.doi.org/10.1021/jm301544x | J. Med. Chem. 2013, 56, 521–533

Scheme 1. Synthesis of the Compounds with Isosteric Replacement of the NO_2 Group[a]

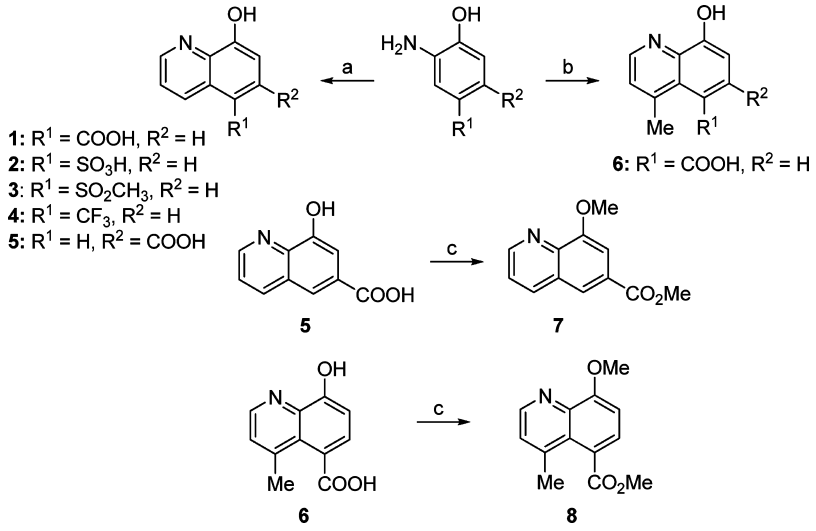

[a]Reagents and conditions: (a) acrolein, 6 M HCl, 100 °C, 1 h; (b) crotonaldehyde, 6 M HCl, 100 °C, 1 h; (c) CH_2N_2, Et_2O, room temp, 1 h.

Scheme 2. Synthesis of the 7-Substituted Nitroxoline Analogues[a]

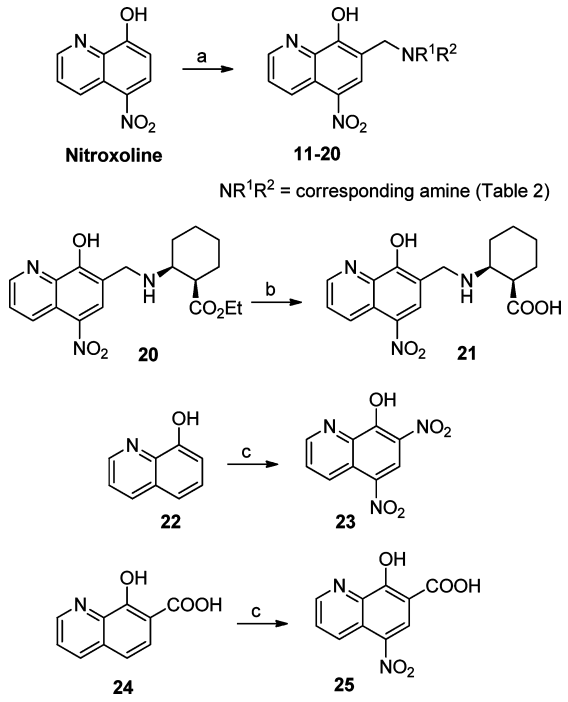

[a]Reagents and conditions: (a) corresponding amine (R^1R^2NH, Table 1), HCHO, Py, 60 °C, 1−24 h; (b) 1 M NaOH, dioxane/H_2O, room temp, 2 h; (c) HNO_3/H_2SO_4, room temp, 3 h.

nitration of 8-hydroxyquinoline-7-carboxylic acid (**24**) (Scheme 2).

3.3. Synthesis of 8-Substituted Derivatives. Several synthetic approaches were used to obtain various 8-substituted nitroxoline derivatives. Four different 8-alkyloxy-5-nitroquinolines were synthesized (Scheme 3). As the alkylation of nitroxoline with 2-bromoacetonitrile was not successful under several conditions, we pursued a different synthetic approach. 8-Hydroxyquinoline (**22**) reacted easily with 1 equiv of 2-bromoacetonitrile in the presence of Cs_2CO_3, which provided the 8-cyanomethoxy product **26** in high yield (91%). After that, an efficient nitration procedure using a KNO_3/H_2SO_4 mixture was applied, which provided the desired product **27** in 85% yield, with only minor amounts of the side product **28**. The amount of **28** was reduced by the minimal amount of sulfuric acid used. The hydrolysis of the cyano group of **27** to the carboxyl derivative **29** was achieved by heating in concentrated HCl for 24 h, and the subsequent conversion to the methyl ester **30** was performed using diazomethane (Scheme 3).

The synthesis of 8-amino-5-nitroquinoline (**32**) proceeded smoothly by the previously described aromatic amination of 5-nitroquinoline, using (**31**) 1,1,1-trimethyhydrazinium iodide (TMHI) and *t*-BuOK in dimethyl sulfoxide (DMSO) (Scheme 4).[36] Starting from the 8-aminoquinoline (**34**), the 8-acetamido-5-nitroquinoline (**36**) was also synthesized. As a side product under these reaction conditions, we concurrently obtained the 5,7-dinitrated 8-aminoquinoline analogue **37** (Scheme 4).

In parallel with these studies an efficient microwave-assisted synthetic procedure for synthesis of the 5-nitro-8-quinolinylamine derivatives was discovered.[37] We revealed that the cyanomethoxy group can serve as a good leaving group for nucleophilic aromatic substitutions in the quinoline system. Several different nitrogen nucleophiles (3 equiv) were thus reacted under microwave conditions (150 W, 15 min to 2 h, MeCN) with 8-cyanomethoxy-5-nitroquinoline (**27**), which has OCH_2CN as a leaving group at position 8 of the quinoline ring (Scheme 5, Table 2). This methodology provided rapid access to different 8-aminonitroxoline analogues **38**−**48** in moderate to high yields.

3.4. Replacing the Quinoline Ring with a Naphthalene Ring. In the last phase, we wanted to determine if the quinoline ring represents an important part of catB inhibitors (with a limited number of compounds). As well as purchasing 4-nitro-1-naphthol (**49**) and 1-amino-4-nitronaphthalene (**50**) to directly compare them with their quinoline analogues (i.e., nitroxoline and compound **32**), we used compound **49** to synthesize two additional derivatives to compare their inhibitory activities with the corresponding compounds from the quinoline series. First, we transformed the hydroxyl group of compound **49** into methylsulfonate **51**, and then we reacted

dx.doi.org/10.1021/jm301544x | J. Med. Chem. 2013, 56, 521−533

Scheme 3. Synthesis of the 8-Alkyloxy Substituted Nitroxoline Analogues[a]

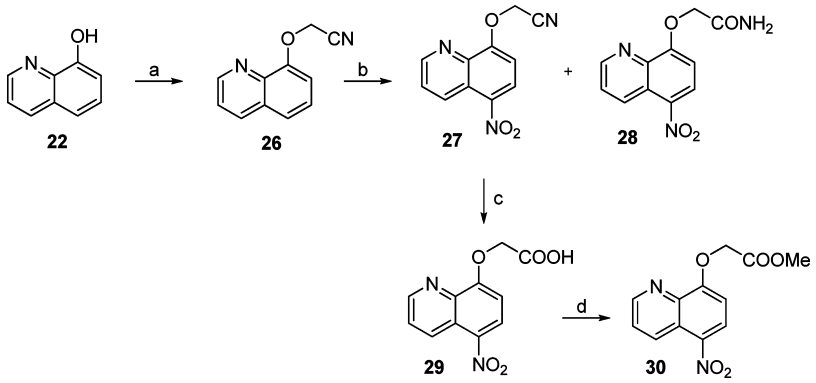

[a]Reagents and conditions: (a) $BrCH_2CN$, Cs_2CO_3, DMSO, room temp, 1 h; (b) KNO_3/H_2SO_4, 0 °C, 15 min, room temp, 1 h; (c) HCl (37%), 60 °C, 24 h; (d) CH_2N_2, Et_2O, room temp, 1 h.

Scheme 4. Synthesis of 8-Amino-5-nitroquinoline (32) and 8-Acetamido-5-nitroquinoline (36)[a]

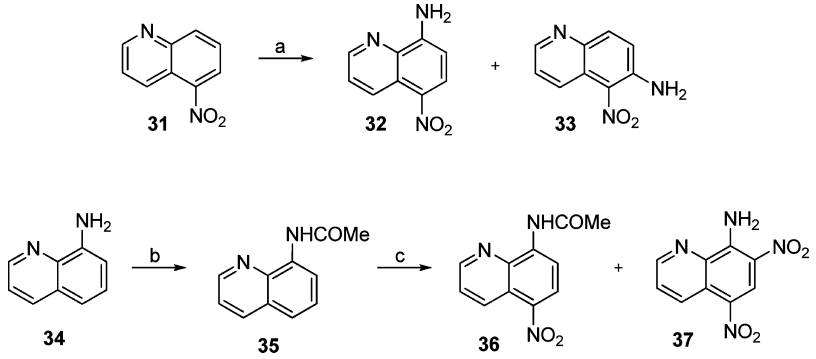

[a]Reagents and conditions: (a) TMHI, *t*-BuOK, DMSO, room temp; (b) Ac_2O, room temp; (c) KNO_3/H_2SO_4, 0 °C to room temp, 5 h.

Scheme 5. Synthesis of 5-Nitro-8-quinolinylamines[a]

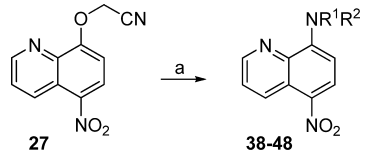

[a]Reagents and conditions: (a) corresponding amine (R^1R^2NH, Table 2), microwave, MeCN, 15 min to 2 h.

this intermediate with either pyrrolidine or morpholine to yield **52** or **53**, respectively (Scheme 6).

Moreover, some structurally distinct derivatives were synthesized (without a quinoline analogue). For example, 1-amino-4-nitronaphthalene (**50**) was used to try to incorporate a cyano moiety into the molecule and to obtain the 1-cyanamide-4-nitronaphthalene. For this purpose, we reacted compound **50** with cyanogen bromide; however, after isolation and purification of the product, we established with NMR and mass spectrometry that bromination at the position ortho with respect to the amino group took place to yield compound **54** (Scheme 6). Nevertheless, we successfully cyanomethylated compound **50** using paraformaldehyde, KCN, and $ZnCl_2$ in CH_3COOH. Both the monocyanomethylated product **55** and the dicyanomethylated product **56** were isolated and purified (Scheme 6). Other compounds included in this series were purchased from commercially available sources (compounds **57** and **58**, Table 3).

4. RESULTS AND DISCUSSION

4.1. Cathepsin B Inhibitory Activities and Enzyme Kinetics. The synthesized compounds were first evaluated for their relative inhibition of catB endopeptidase and exopeptidase activities, using the catB specific substrates Z-Arg-Arg-7-amido-4-methylcoumarin (Z-Arg-Arg-AMC) and 2-aminobenzoyl (Abz)-Gly-Ile-Val-Arg-Ala-Lys(Dnp)-OH, respectively (results not shown). The compounds that showed relative inhibitions similar to nitroxoline at 50 μM (endopeptidase activity, 21.9% ± 3.3%; exopeptidase activity, 24.7% ± 2.8%) were further carefully characterized by determining their kinetic parameters and their mode of inhibition. The exact protocols are described in the section Materials and Methods.

Nitro-substituted benzene derivatives are associated with toxicity that is a consequence of partial reduction to the hydroxylamine, which can then undergo metabolic activation to an electrophilic nitroso species.[34] For this reason and to evaluate the importance of the NO_2 group for catB inhibition, we replaced the NO_2 functionality with its (bio)isosteric surrogates: a carboxyl group (compound **1**), sulfonic acid (compound **2**), a methylsulfonyl group (compound **3**), a trifluoromethyl group (compound **4**), a carboxymethyl group (compound **8**), fluorine (compound **9**), and the ring nitrogen (compound **10**). This last was used, as it is known that pyridine is the most common aromatic NO_2 isostere. Moreover, the positions of the carboxyl and the carboxymethyl groups were also varied (from 5-substituted to 6-substituted compounds, **5** and **7**) to see if the position on the ring has any role. It was

dx.doi.org/10.1021/jm301544x | J. Med. Chem. 2013, 56, 521−533

Scheme 6. Synthesis of the Naphthalene Derivatives[a]

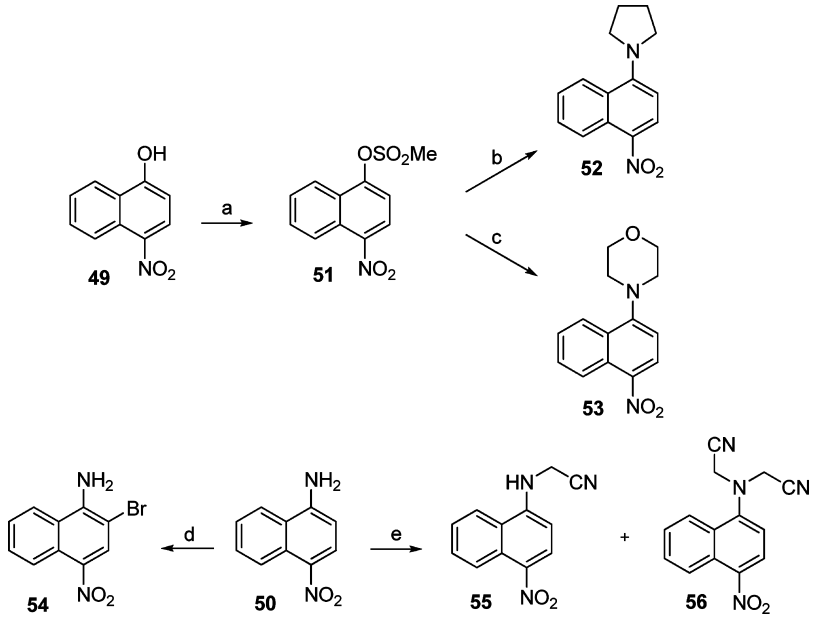

[a]Reagents and conditions: (a) $MeSO_2Cl$, Et_3N, CH_2Cl_2, room temp; (b) pyrrolidine, EtOH, microwave, 100 °C, 20 min; (c) morpholine, EtOH, microwave, 100 °C, 10 min; (d) BrCN, THF; (e) $(CH_2O)_n$, KCN, $ZnCl_2$, CH_3COOH, H_2SO_4, 55 °C.

previously established that the absence of the NO_2 group of position 5 on a quinoline ring leads to a loss of catB inhibition (compound **22**, Table S1, Supporting Information)[31] and that replacing the nitro group with an amino moiety leads to a switch from catB-specific inhibition to redox-based nonspecific inactivation of cysteine cathepsins.[38] The results presented in Table S1 show that replacing the nitro group with the substituents used in this study leads to a loss of catB inhibition (Table S1), confirming the findings of our previous study; hence, the NO_2 group at position 5 is a prerequisite for catB inhibition.

On the basis of the cocrystal structure of nitroxoline with catB,[31] we hypothesized that substituents attached to position 7 of 5-nitro-8-hydroxyquinoline would extend into the S1′ subsite and thus contribute to the binding affinity and enhance catB inhibition. For this reason, 7-aminomethylated derivatives **11**−**21** were synthesized and evaluated for catB inhibition. As the S1′ subsite favors hydrophobic interactions,[39,40] lipophilic moieties were predominantly used at position 7 of the quinoline ring.

Most of the 7-aminomethylated derivatives **11**−**21** showed the same mode of catB endopeptidase inhibition as for nitroxoline (Table 1), i.e., a mixed type of inhibition with a predominantly uncompetitive component. The K_i' values for the dissociation of the enzyme−substrate−inhibitor complex were in most cases lower than the K_i values for the dissociation of the enzyme−inhibitor complex. Therefore, we can postulate that these derivatives bind to the enzyme−substrate complex with a higher affinity than to the free enzyme. Also, the inhibitory activities of the catB endopeptidase function remained in the same concentration range as for the parent nitroxoline. The only exceptions to this rule were compounds **15** and **17**, which inhibited catB as uncompetitive inhibitors with improved inhibition over nitroxoline.

When using Abz-Gly-Ile-Val-Arg-Ala-Lys(Dnp)-OH as the substrate for the catB exopeptidase activity, most of the 7-substituted derivatives **11**−**21** showed the same mode of inhibition as nitroxoline, i.e., noncompetitive. The only two exceptions were compounds **15** and **21**, where the former showed mixed inhibition and the latter showed competitive inhibition of the catB exopeptidase activity. Moreover, these derivatives were all similarly potent inhibitors of catB exopeptidase activity as nitroxoline, with K_i values ranging from 130 to 360 μM (Table 1).

Interestingly, 7-substituted nitroxoline derivatives that have either an NO_2 (**23**) or a COOH (**25**) group at this position showed uncompetitive inhibition of catB endopeptidase activity (Table 1). Similar to nitroxoline, compound **23** showed 2-fold selectivity for inhibition of the endopeptidase activity (K_i = 72 ± 8 μM, Table 1). Although the inhibition of catB exopeptidase activity of compound **25** was not pronounced (K_i = 221 ± 33 μM, Table 1), it is very interesting that this compound (**25**) showed a competitive mechanism of inhibition.

Taken together, the most promising compound of this series proved to be compound **17**. When using Z-Arg-Arg-AMC as a substrate, compound **17** acted as an uncompetitive inhibitor of catB, with a K_i' of 5 ± 1 μM (8-fold improvement over nitroxoline). Additionally, it showed 85-fold selectivity for inhibition of the endopeptidase activity and thus represented the most suitable candidate molecule for investigation in the biological assays.

In agreement with our previous study that showed that removal of the hydroxyl group from position 8 of the 5-nitroquinoline ring resulted in significantly lower catB inhibition (compound **31**, Table S3, Supporting Information),[31] the 8-alkyloxy substituted nitroxoline derivatives assayed here also led to diminished activity (compounds **27**−**30**, Table S2, Supporting Information). Similarly, 8-amino-5-nitroquinoline (**32**), 6-amino-5-nitroquinoline (**33**), 8-acetamido-5-nitroquinoline (**36**), and 5,7-dinitro-8-aminoquinoline (**37**) showed lower catB endopeptidase inhibition when compared with nitroxoline (for compounds **32**, **33**, **36**, and **37**, see Table S3, Supporting Information). On the basis of the docking experiments (not shown), we postulate that larger

dx.doi.org/10.1021/jm301544x | J. Med. Chem. 2013, 56, 521−533

Table 1. Cathepsin B Inhibitory Activities of 7-Substituted Nitroxoline Derivatives

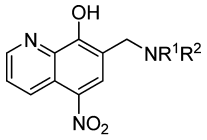

11-21

	HNR^1R^2	Z-Arg-Arg-AMC		Abz-Gly-Ile-Val-Arg-Ala-Lys(Dnp)-OH	
		K_i (μM)[a]	K_i' (μM)[a]	K_i (μM)[a]	K_i' (μM)[a]
11	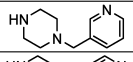	311 ± 54[b]	171 ± 26[b]	364 ± 46[c]	
12	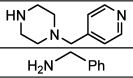	143 ± 28[b]	94 ± 9[b]	162 ± 18[c]	
13	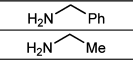	198 ± 63[b]	58 ± 0[b]	154 ± 15[c]	
14		117 ± 23[b]	82 ± 17[b]	136 ± 12[c]	
15	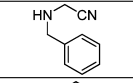	-	19 ± 3[d]	79 ± 24[b]	8 ± 2[b]
16	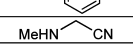	126 ± 40[b]	76 ± 16[b]	172 ± 16[c]	
17	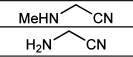	-	5 ± 1[d]	426 ± 39[c]	
18	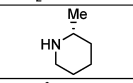	203 ± 5[b]	116 ± 11[b]	243 ± 21[c]	
19	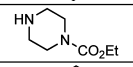	129 ± 3[b]	87 ± 2[b]	156 ± 12[c]	
20	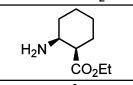	132 ± 21[b]	74 ± 0[b]	130 ± 0[c]	
21	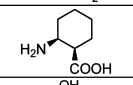	181 ± 20[b]	125 ± 16[b]	250 ± 93[e]	-
23	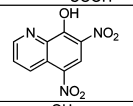	-	72 ± 8[d]	146 ± 26[c]	
25	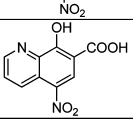	-	117 ± 10[d]	221 ± 33[e]	-

[a] K_i and K_i' values are the mean ± SD (n = 4). [b] Mixed inhibition. [c] Noncompetitive inhibition. [d] Uncompetitive inhibition. [e] Competitive inhibition.

substituents are needed at position 8 of the 5-nitroquinoline, as they can then extend into the S1 and/or S2 subsite of the active site. Therefore, we synthesized several 5-nitro-8-quinolinylamines (compounds **38**−**48**, Table 2) to clarify the role of different substituents at this position.

A general trend from the inhibition assay results of the 5-nitro-8-quinolinylamines **38**−**48** (Table 2) is that these compounds are weaker endopeptidase inhibitors than nitroxoline, although they showed better inhibition when Abz-Gly-Ile-Val-Arg-Ala-Lys(Dnp)-OH was used as the substrate. The most potent exopeptidase activity inhibitor was compound **42**, with a K_i of 24 ± 1 μM (more than 10-fold lower compared with nitroxoline). It is possible that the 4-methylpiperidine moiety binds in the S1 or S2 pocket of the active site of catB, and this can contribute to an improved binding affinity. It is known that the S1 and S2 subsites prefer hydrophobic and basic residues.[39,40] This might explain the slightly improved results obtained for compounds with saturated rings (**41**−**44**) or pyridine (**47**) attached at position 8, in comparison with compounds with a benzyl moiety (**45**, **46**, **48**) (Table 2). From a comparison of the inhibitory activities of compounds **40**, **41**, **42**, and **43**, we can postulate that larger saturated hydrophobic moieties at position 8 of the 5-nitroquinoline ring are preferred for improved inhibition of exopeptidase activity. The detailed kinetic analyses showed that 5-nitro-8-quinolinylamine derivatives act as noncompetitive inhibitors of catB exopeptidase activity (with the exception of compounds **44** and **46**, which acted as mixed and competitive inhibitors, respectively).

From the assay results of the compounds with a naphthalene ring presented in Table 3, we see that removal of the ring nitrogen had an influence on the potency; e.g., 4-nitro-1-naphthol (**49**) was approximately 2-fold less potent than nitroxoline, although it retained the same mode of inhibition. Conversely, 1-amino-4-nitronaphthalene (**50**) showed very similar inhibitory properties of both catB activities when compared with its quinoline counterpart, compound **32** (Table S3). Through comparing compounds **52** and **53** with **40** and **41**, we can postulate that the quinoline replacement does not impair the inhibition of endopeptidase activity, as this stays approximately the same. However, there was an improvement in the catB exopeptidase inhibition with the naphthalene derivative **53** (K_i = 85 ± 9 μM, Table 3), in comparison to compound **41** (K_i = 155 ± 10 μM, Table 2), and also derivative **52** (K_i = 34 ± 5 μM, Table 3) in comparison to compound **40** (no inhibition observed, Table 2).

The most promising compound from this series was compound **54**, which showed almost 7-fold selectivity for inhibition of the endopeptidase activity. The kinetic studies

dx.doi.org/10.1021/jm301544x | J. Med. Chem. 2013, 56, 521−533

Table 2. Cathepsin B Inhibitory Activities of 5-Nitro-8-quinolinylamines

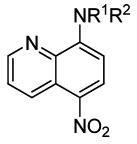

38-48

	HNR^1R^2	Z-Arg-Arg-AMC		Abz-Gly-Ile-Val-Arg-Ala-Lys(Dnp)-OH	
		K_i (μM)[a]	K_i' (μM)[a]	K_i (μM)[a]	K_i' (μM)[a]
38	$(Me)_2NH\times HCl$	NI		NI	
39	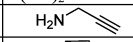	NI		NI	
40		NI		NI	
41		180 ± 2[b]	153 ± 16[b]	155 ± 10[c]	
42	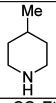	207 ± 2[b]	105 ± 7[b]	24 ± 1[c]	
43	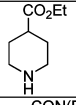	162 ± 6[b]	113 ± 18[b]	38 ± 3[c]	
44	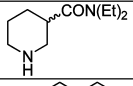	155 ± 18[b]	117 ± 2[b]	105 ± 5[b]	36 ± 13.6[b]
45	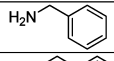	349 ± 42[b]	127 ± 21[b]	364 ± 60[c]	
46	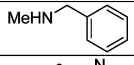	242 ± 43[b]	137 ± 1[b]	196 ± 30[e]	-
47	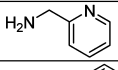	107 ± 18[b]	87 ± 12[b]	47 ± 4[c]	
48	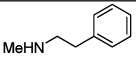	-	175 ± 9[d]	350 ± 27[c]	

[a] K_i and K_i' values are the mean ± SD (n = 4). NI: no inhibition. [b] Mixed inhibition. [c] Noncompetitive inhibition. [d] Uncompetitive inhibition. [e] Competitive inhibition.

Table 3. Cathepsin B Inhibitory Activities of Naphthalene Derivatives

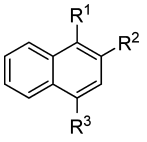

49, 50, 52-58

	R^1	R^2	R^3	Z-Arg-Arg-AMC		Abz-Gly-Ile-Val-Arg-Ala-Lys(Dnp)-OH	
				K_i (μM)[a]	K_i' (μM)[a]	K_i (μM)[a]	K_i' (μM)[a]
49	OH	H	NO_2	373 ± 176[b]	84 ± 6[b]	NI	
50	NH_2	H	NO_2	217 ± 46[b]	111 ± 12[b]	147 ± 4[c]	
52		H	NO_2	170 ± 45[b]	277 ± 11[b]	34 ± 5[c]	
53	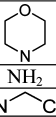	H	NO_2	289 ±37[b]	125 ± 34[b]	85 ± 9[c]	
54	NH_2	Br	NO_2	-	32 ± 14[d]	212 ± 46[c]	
55	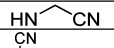	H	NO_2	NI		NI	
56	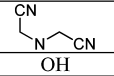	H	NO_2	NI		NI	
57	OH	H	SO_3H	NI		n.d.	
58	NH_2	OH	SO_3H	NI		n.d.	

[a] K_i and K_i' values are the mean ± SD (n = 4). NI: no inhibition. n.d.: not determined. [b] Mixed inhibition. [c] Noncompetitive inhibition. [d] Uncompetitive inhibition.

dx.doi.org/10.1021/jm301544x | J. Med. Chem. 2013, 56, 521−533

demonstrated that compound **54** acts as an uncompetitive inhibitor, with a K_i of 32 ± 14 μM. Of great interest, compound **52** showed a 5-fold preference for catB exopeptidase inhibition over its endopeptidase activity. Although this compound is most probably not suitable for further development of catB inhibitors, it can be used as a research tool to help to elucidate the role of catB in physiological and pathological processes, as proposed previously for catB inhibitors that primarily target the catB exopeptidase activity.[41]

Nitrile-containing inhibitors of the cysteine cathepsins that form reversible covalent interactions with the active site thiol have received growing interest over the past decade.[30] As evident from the cocrystal structure of nitroxoline in the catB active site,[31] we predicted that positions 7 and 8 on the quinoline ring are in the proximity of the catalytic Cys29. Moreover, these positions also offer the possibility of straightforward chemical modifications, and they are thus suitable for the introduction of this mildly electrophilic "warhead". The small series of nitroxoline derivatives presented here contained the nitrile moiety (compounds **15**−**17**, **27**, **55**, **56**). Although the inhibitory activities of these synthesized derivatives improved in some cases (e.g., compounds **15** and **17**), it appears that this was not a consequence of a covalent reaction, as the literature data show that the K_i values are significantly lower when the cysteine is involved in a covalent reaction.[30]

As it is unclear whether micromolar-range enzyme inhibitors are potent enough to be considered as potential drug candidates for anticancer therapy, the best performing compound from the series (compound **17**) was further evaluated in functional in vitro tests using the human transformed cell line MCF-10A neoT (see section 4.3). At this point, it is also appropriate to emphasize the low molecular weight of the inhibitors presented here. This fact renders them appropriate for further optimization and improvement of their potency in order to obtain compounds that are even more suitable as potential drug candidates.

4.2. Cathepsin B Selectivity. The selective catB endopeptidase inhibitors **17** and **54** and the selective catB exopeptidase inhibitors **42** and **52** were chosen as the most promising among these compounds. To assess their selectivity toward catB, two additional cysteine proteases, cathepsin H (catH, EC 3.4.22.16) and cathepsin L (catL, EC 3.4.22.15) were chosen because of their distinct mechanisms of enzymatic cleavage. Whereas catH cleaves substrates as an amino- and endopeptidase, catL acts as an endopeptidase.[2] These compounds showed a preference for catB inhibition over catH and catL inhibition. Compound **17** was the most selective, as it showed 24-fold and 23-fold greater preference for inhibition of catB over catH and catL, respectively (Table 4).

Table 4. Inhibition Constants of Selected Compounds against Cathepsins H and L

	cathepsin H, R-AMC		
compd	K_i (μM)[a]	K_i' (μM)[a]	cathepsin L, Z-FR-AMC, K_i (μM)[a]
17	129 ± 6[b]	129 ± 6[b]	124 ± 3[c]
42	221 ± 37[b]	221 ± 37[b]	155 ± 0[c]
52		251 ± 33[d]	245 ± 6[c]
54		354 ± 37[d]	182 ± 4[c]

[a]K_i and K_i' values are the mean ± SD (n = 4). [b]Noncompetitive inhibition. [c]Competitive inhibition. [d]Uncompetitive inhibition.

Compound **42** showed 9-fold and 6-fold greater preference for inhibition of catB over catH and catL, respectively. A similar trend was seen with compounds **52** and **54**, which showed 7-fold and 11-fold greater preference for inhibition of catB over catH and concurrently a more than 6-fold greater inhibition of catB over catL. In general, these compounds showed improved selectivity toward catB over the parent compound nitroxoline, which was previously shown to have a 7.4-fold and 4.8-fold greater preference for inhibition of catB over catH and catL, respectively.[31]

4.3. In Vitro Anticancer Activity. CatB has been shown to be substantially involved in the progression of cancers through its facilitation of the intracellular and extracellular degradation of ECM proteins.[10,18] To assess the ability of the best of these compounds in the presented series (compound **17**) to impair these deleterious processes, MCF-10A neoT cells (c-Ha-ras-transformed human breast epithelial cells) and the quenched fluorescent substrate DQ-collagen IV were used. Collagen IV is a major constituent of basement membranes,[42] and this fluorescein-labeled derivative of collagen IV shows bright green fluorescence after enzymatic cleavage. As shown previously,[18,19,31] the MCF-10A neoT cells degraded DQ-collagen IV intracellularly and extracellularly (Figure 3A).

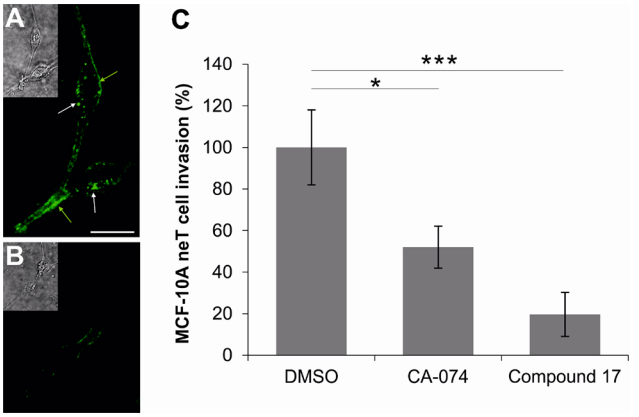

Figure 3. Compound **17** inhibits DQ-collagen IV degradation and tumor cell invasion of MCF-10A neoT cells. (A) MCF-10A neoT cells degrade DQ-collagen IV intracellularly (white arrows) and extracellularly (green arrows), as shown under fluorescence microscopy. (B) Addition of compound **17** (5 μM) impairs intracellular and extracellular DQ-collagen IV degradation. (A, B) Main panels are images of green fluorescence following hydrolysis of DQ-collagen IV (scale bar, 20 μm), and the smaller inserted panels are transmission images. (C) Compounds **17** (5 μM) and CA-074 (5 μM) significantly abrogated MCF-10A neoT cell invasion in the xCELLigence system. The results are the mean ± SD (n = 4) and are representative of two independent experiments: (*) $P < 0.05$, (***) $P < 0.001$, relative to DMSO control (two-tailed Student's t-test).

While the latter is associated with pericellular forms of cathepsin B (bound to the cell surface or exocytosed in the extracellular milieu), the former is associated with lysosomal cathepsin B, which degrades the endocytosed and partially degraded ECM. Previous studies have shown that the sole inhibition of the extracellular catB is not enough for significant attenuation of tumor cell invasion and that the intracellular catB inhibition is also needed to efficiently impair tumor cell invasion[43] and angiogenesis.[44] Therefore, there is a great need for cell-permeable inhibitors of catB that are able to cross cell membranes and inhibit the intracellular catB. Here, the addition

dx.doi.org/10.1021/jm301544x | J. Med. Chem. 2013, 56, 521−533

of compound **17** to the cell medium (final concentration, 5 μM) attenuated both the intracellular and extracellular DQ-collagen IV degradation, as shown under fluorescence microscopy (Figure 3B) indicating that compound **17** possesses the desired cell-permeable characteristics.

As ECM degradation is a prerequisite for tumor invasion, we postulated that compound **17** might also be effective in the blocking of tumor-cell invasion. For this purpose, we used an in vitro invasion model: the xCELLigence system. This is a two-chamber-based system, with the chambers separated by a porous membrane coated with a layer of matrix that mimics the ECM. The xCELLigence system allows real-time monitoring of cells that degrade the ECM barrier and migrate to the lower chamber. By use of this system, compound **17** (final concentration, 5 μM) was shown to significantly abrogate the invasion of MCF-10A neoT cells (80% ± 11%), compared to the DMSO control (Figure 3C). As a positive control, an irreversible catB-specific inhibitor CA-074 (final concentration, 5 μM, previously shown to be nontoxic[18]) was used. CA-074 significantly inhibited MCF-10A neoT cell invasion (48 ± 10%) when compared to DMSO (Figure 3C). These values are in line with the previous reports showing that the inhibition of catB cannot completely impair the invasiveness of tumor cells because of the induction of other proteases providing alternative invasion mechanisms.[45] The CA-074 effect on MCF-10A neoT cell invasion was weaker when compared to compound **17**, albeit not significantly. Lower inhibition of CA-074 can be attributed to the nature of its mechanism of action: as an irreversible inhibitor its concentration might become depleted during the 3-day invasion assay. Furthermore, its ionic and peptidic nature renders it cell-impermeable, penetrating the cell membrane only after prolonged exposure,[43] whereas compound **17** displays cell permeable characteristics (Figure 3B).

To exclude the possibility that attenuation of ECM degradation and tumor cell invasion are due to cytotoxic effects of compound **17**, cell viability studies were also performed using the xCELLigence system. MCF-10A neoT cells were incubated with compound **17** at 2.5 and 5 μM, and the cell viability was continuously monitored at 15 min intervals for up to 3 days. Compound **17** did not show significant effects on MCF-10A neoT cell viability up to the third day of measurements, where it slightly increased cell proliferation (113% ± 6% and 117% ± 7% at 2.5 and 5 μM, respectively; Supporting Information, Figure S1). This thus eliminated the possibility that the reduction in ECM degradation and tumor cell invasion resulted from cytotoxicity induced by compound **17** itself.

5. CONCLUSIONS

We synthesized a focused library of nitroxoline derivatives with the aim of exploring the structure−activity relationships for catB endopeptidase and exopeptidase activity inhibition. The best performing and the most promising inhibitor was discovered among the 7-aminomethylated derivatives. Compound **17** that has a 7-CH_2NHCH_2CN moiety showed significantly improved catB endopeptidase inhibition, along with improved selectivity toward catB over catH and catL, in comparison with the parent nitroxoline. Its efficacy was demonstrated in tumor-cell-based assays, where it significantly inhibited extracellular and intracellular degradation of ECM and tumor-cell invasion.

Essentially, most of the compounds presented here have very low molecular weights (e.g., compound **17** has a molecular weight of only 258), and therefore, they have a very beneficial binding efficiency index, one of the indices for assessing ligand efficiency.[46] It is widely known that these indices are very useful for effective compound optimization, as solely taking into account the potency against the target often leads to the neglecting of the physical properties of the compounds being optimized. As a consequence, many such compounds have extremely high molecular weights (one of the key parameters to be considered) very early in the hit or lead optimization process.

Therefore, we are certain that inhibitors of the structural type presented in our manuscript have importance in the field, provide a solid foundation for further structure-based development of catB inhibitors, and are at the moment appropriately balanced in terms of potency and molecular weight.

6. EXPERIMENTAL SECTION

6.1. Materials and Methods. Chemistry. Reagents and solvents were obtained from commercial sources (Fluka, Sigma-Aldrich, Acros Organics, Alfa Aesar, Fluorochem, TCI). Compound **9** was purchased from TCI Chemicals, compound **10** from Synchem, compound **49** from Alfa Aesar, and compounds **50**, **57**, and **58** from Sigma Aldrich. Their identities were confirmed using ^{1}H NMR (see Supporting Information for details) and mass spectrometry prior to use in the biochemical assays. Solvents were distilled before use, while the other chemicals were used as received. All of the reactions were carried out under an argon atmosphere with magnetic stirring, unless otherwise stated. Microwave-assisted reactions were performed using a focused microwave reactor (Discover, CEM Corporation, Matthews, NC, U.S.). Analytical TLC was performed on Merck silica gel (60F254) precoated plates (0.25 mm). The compounds were visualized under UV light and/or stained with the relevant reagent. Column chromatography was performed on Merck silica gel 60 (mesh, 70−230), using the indicated solvents. Yields refer to the purified products, and they were not optimized. All of the melting points were determined on a Reichert hot-stage apparatus and are uncorrected. Optical rotation was measured on a Perkin-Elmer 1241 MC polarimeter. ^{1}H NMR spectra were recorded on a Bruker Avance 400 DPX and a Bruker Avance III 500 DPX spectrometer at 302 K and are reported in ppm using tetramethylsilane or solvent as an internal standard (DMSO-d_6 at 2.50 ppm, $CDCl_3$ at 7.26 ppm). The coupling constants (J) are given in Hz, and the splitting patterns are designated as follows: s, singlet; bs, broad singlet; d, doublet; dd, double doublet; t, triplet; m, multiplet. ^{13}C NMR spectra were recorded on a Bruker Avance 400 DPX and a Bruker Avance III 500 DPX spectrometer at 302 K and are reported in ppm using solvent as an internal standard. Mass spectra data and high-resolution mass measurements were performed on a VG-Analytical Autospec Q mass spectrometer. Elemental analyses were performed on a 240 C Perkin-Elmer C, H, N analyzer. The purity of all new compounds was determined by elemental analyses and the purity of some compounds by HPLC. Analyses indicated by the symbols of the elements were within ±0.4% of the theoretical values (unless noted otherwise in the Supporting Information). HPLC analyses were run on an Agilent 1100 system equipped with a quaternary pump and a multiple wavelength detector. An Agilent Eclipse C18 column (4.6 mm × 50 mm, 5 mm) was used, with a flow rate of 1.0 mL/min, detection at 254 nm, and an eluent system of A, H_2O with 0.1% TFA, and B, MeOH. The following gradient was applied: 0−3 min, 40% B; 3−18 min, 40% B → 80% B; 18−23 min, 80% B; 23−30 min, 80% B → 40% B; run time, 30 min; temperature, 25 °C. The purity of the compounds was >95%, as determined by HPLC.

6.2. Enzymes and Assay Buffers. Human recombinant catB was prepared as reported previously.[47] Human native catH was isolated from human liver,[48] and human recombinant catL was expressed in *Escherichia coli*.[49] The catB endopeptidase and exopeptidase assay

dx.doi.org/10.1021/jm301544x | J. Med. Chem. 2013, 56, 521−533

buffers were 100 mM phosphate buffer, pH 6.0, and 60 mM acetate buffer, pH 5.0,respectively. The assay buffers for catL and catH were 100 mM acetate buffer, pH 5.5, and 100 mM phosphate buffer, pH 6.8, respectively. Each of these buffers contained 0.1% PEG 8000 (Sigma-Aldrich), 5 mM DTT, and 1.5 mM EDTA. Prior to the assays, each enzyme was activated in the respective assay buffer for 5 min at 37 °C.

6.3. Determination of Relative Inhibition. The substrates Z-Arg-Arg-AMC (Calbiochem) and Abz-Gly-Ile-Val-Arg-Ala-Lys(Dnp)-OH (Bachem) were used to assess the endopeptidase and exopeptidase activities of catB, respectively. Five microliters of the substrate (final concentrations of 5 and 1 μM for endopeptidase and exopeptidase substrates, respectively) and 5 μL of the respective compounds (for a 50 μM final concentration) were added into the wells of a black microplate. The reaction was initiated by addition of 90 μL of catB in the assay buffer (final concentrations of 5 and 0.5 nM for the endopeptidase and exopeptidase activities, respectively). Formation of the fluorescent degradation product of the AMC substrate was continuously monitored at 37 °C at 460 nm (±10 nm), with excitation at 380 nm (±20 nm). For Abz-Gly-Ile-Val-Arg-Ala-Lys(Dnp)-OH, the formation of the fluorescent degradation product was monitored at 37 °C at 420 nm (±10 nm), with excitation at 320 nm (±20 nm). All of the assay mixtures contained 5% (v/v) DMSO and 0.01% Triton X-100 to prevent false-positive inhibition due to the formation of compound aggregates.[50] All of the measurements were performed twice, each of which was in duplicate. The relative inhibition of the enzyme activities was calculated according to the following equation: Relative inhibition (%) = $100(1 - v_i/v_o)$, where v_i and v_o denote the reaction velocity in the presence and absence of inhibitor, respectively.

6.4. Determination of K_i Values. Inhibition constants were determined by measuring the reaction velocities at various substrate concentrations in the presence of increasing concentrations of the inhibitors. Five microliters of substrate at three concentrations and 5 μL of the inhibitor at seven final concentrations (0, 20, 40, 60, 80, 100, and 200 μM) were added to wells of a black microplate. The reaction was initiated with 90 μL of enzyme in the assay buffer. Substrates Z-Arg-Arg-AMC (Calbiochem) at 60, 180, and 360 μM and Abz-Gly-Ile-Val-Arg-Ala-Lys(Dnp)-OH (Bachem) at 1, 3, and 6 μM were used for assessing catB endopeptidase and exopeptidase activities, respectively. The K_m values for both substrates were determined in separate experiments and were 346.1 μM (R^2 = 0.9995) for Z-Arg-Arg-AMC and 6.3 μM (R^2 = 0.9694) for Abz-Gly-Ile-Val-Arg-Ala-Lys(Dnp)-OH. Substrates Arg-AMC (Biomol) at 20, 80, and 160 μM and Z-Phe-Arg-AMC (Bachem) at 0.5, 1, and 4 μM were used for assessing the K_i values of compound **17** against catH and catL. Formation of the fluorescent degradation products was monitored as above. All assay mixtures contained 5% (v/v) DMSO. All measurements were performed twice, with each in duplicate. The resulting data were analyzed by nonlinear regression using the SigmaPlot 12 software and were fitted to models for competitive, noncompetitive, uncompetitive, and mixed type enzyme inhibition, as provided with the software. The mode of inhibition and K_i values were chosen from the best ranking model, as determined by the software. A representative graph depicting the data fit for the best ranking model of inhibition for compound **16** is shown in the Supporting Information (Figure S1).

6.5. Cell Culture. MCF-10A neoT, a c-Ha-Ras oncogene transfected human breast epithelial cell line, was provided by Bonnie F. Sloane (Wayne State University, Detroit, MI, U.S.). These MCF-10A neoT cells were cultured in DMEM/F12 (1:1) medium (Gibco) supplemented with 5% fetal bovine serum (HyClone), 1 μg/mL insulin (Sigma-Aldrich), 0.5 μg/mL hydrocortisone (Sigma-Aldrich), 50 ng/mL EGF (Sigma-Aldrich), 2 mM glutamine (Gibco), and antibiotics at 37 °C in a humidified atmosphere of 5% CO_2. Prior to their use in the assays, the cells were detached from the culture flasks using 0.05% trypsin (Gibco) and 0.02% EDTA in phosphate buffered saline, pH 7.4.

6.6. Cell-Viability Assay. To evaluate the potential cytotoxic effects of compound **17** on MCF-10A neoT cells, the xCELLigence system (Roche) was used. The system monitors cellular events in real time; i.e., it measures the electrical impedance (expressed as cell index) generated by cells attached to the bottom of the wells, which have integrated electrodes. MCF-10A neoT cells (7500 cells in 150 μL of medium/well) were seeded into the wells of an E-plate 16 (Roche), following the xCELLigence real time cell analyzer DP instrument manual, as provided by the manufacturer (Roche). The cell index (CI) was monitored every 15 min, and after ~10 h when the cells were in the log growth phase, 50 μL of compound **17** in medium (final concentrations of 2.5 and 5 μM) or the suitable control (0.2% DMSO in medium) was added, and the experiments were run for 72 h. During the course of the experiments (once in every 24 h), the medium was replaced with fresh medium containing the inhibitor or suitable control to prevent cell death due to medium depletion.

6.7. DQ-Collagen IV Degradation. Wells of cooled Lab-Tek chambered coverglass (Nalge Nunc International) were coated with 25 μg/mL DQ-collagen IV (Invitrogen) suspended in 40 μL of 100% Matrigel. Then an amount of 400 μL of MCF-10A neoT cells (6×10^4 cells/mL) was plated onto the gelled Matrigel in medium containing 2% Matrigel and compound **17** (5 μM) or DMSO (0.05%). After 24 h the samples were monitored for fluorescent degradation products using an Olympus IX 81 motorized inverted microscope and Cell^R software.

6.8. Invasion Assay. The two-dimensional invasion assay of MCF-10A neoT cells was monitored using the xCELLigence real time cell analyzer as described previously,[51] with minor modifications. The well-bottoms of 16-well CIM plates (CIM-16 plates, Roche) were coated with 0.3 μg of fibronectin from bovine plasma (Calbiochem). The upper compartments of CIM-16 plates were coated with a thick layer (20 μL per membrane) of 5 mg/mL Matrigel in serum-free medium (BD Biosciences) and allowed to gel for 20 min at 37 °C. After 20 min, the lower compartments were filled with 180 μL of medium containing compound **17** (5 μM) or the suitable control (0.05% DMSO), and the top and bottom portions of the CIM-16 plates were assembled together. The assembled CIM-16 plates were allowed to equilibrate for 30 min at 37 °C in a 5% CO_2 atmosphere after the addition of 60 μL of serum-free medium with compound **17** (5 μM) or DMSO (0.05%) to the wells of the top chamber. Then 80 μL of MCF-10A neoT cell suspension (3×10^4 cells/well) was seeded into the top chambers of the assembled CIM-16 plates, which were placed into the xCELLigence system for data collection. The xCELLigence software was set to collect impendence data (reported as cell index) every 15 min from the time of plating until the end of the experiment (72 h). The data were analyzed with the real time cell analyzer software (Roche), and the percentages of invasion were calculated as the ratio of the cell index of invaded cells in the presence of compound **17** to the cell index of invaded cells in the presence of DMSO.

6.9. Experimental Procedures. *6.9.1. General Procedure for the Synthesis of 7-Aminomethylated Nitroxoline Derivatives **11**–**20**: The Mannich Reaction.* 7-Aminomethylated derivatives of nitroxoline were synthesized under the Mannich reaction conditions according to the known literature procedure.[35] To a stirred and heated (60 °C) solution of 5-nitro-8-hydroxyquinoline (1 equiv) in pyridine (20 mL), an aqueous solution of formaldehyde (≥36.5%, 1 mL) and the desired amine (1 equiv) were added. After heating the reaction mixture to 60 °C until the reaction was complete, it was cooled to room temperature and the product filtered off and washed with cold EtOH (2× 20 mL). Compounds **11**–**20** were subsequently purified by crystallization or column chromatography.

*2-(Benzyl((8-hydroxy-5-nitroquinolin-7-yl)methyl)amino)-acetonitrile (**15**).* The compound was purified by column chromatography (CH_2Cl_2/MeOH, 15/1) and subsequent crystallization from EtOH. Yield, 74% (1.29 g); orange crystals (prisms); mp 110.0–112.5 °C; IR (KBr) υ = 3277, 3026, 2858, 2814, 2228, 1570, 1534, 1505, 1460, 1418, 1305, 1242, 1168, 1129, 1115, 1976, 979, 916, 852, 795, 748, 728, 701, 686, 652, 639 cm^{-1}; ^1H NMR (400 MHz, DMSO-d_6) δ 3.67 (s, 2H, CH_2), 3.74 (s, 2H, CH_2), 3.94 (s, 2H, CH_2), 7.24–7.39 (m, 5H, Ar-H), 7.88 (dd, J = 9.0, 4.5 Hz, 1H, Ar-H), 8.63 (s, 1H, Ar-H), 9.00 (dd, J = 4.0, 1.5 Hz, 1H, Ar-H), 9.17 (dd, J = 9.0, 1.5 Hz, 1H, Ar-H); ^{13}C NMR (100 MHz, DMSO-d_6) δ 41.5, 50.4, 57.3, 115.7, 118.9, 121.6, 125.1, 127.5, 128.5, 128.7, 129.4, 132.8, 134.3, 136.9,

dx.doi.org/10.1021/jm301544x | J. Med. Chem. 2013, 56, 521–533

137.2, 148.9, 158.6; HRMS (ESI) m/z calculated for $C_{19}H_{17}N_4O_3$ $[M + H]^+$ 349.1301, found 349.1305. Anal. ($C_{19}H_{16}N_4O_3$) C, H, N.

*2-(((8-Hydroxy-5-nitroquinolin-7-yl)methyl)amino)acetonitrile (**17**).* **17** was synthesized according to the general procedure. The solid obtained was resuspended in methanol and mixed for 5 h. The undissolved residue was then filtered off and the filtrate evaporated. The compound was subsequently purified by column chromatography (CH_2Cl_2/MeOH, 20/1). Yield, 56% (610 mg); orange solid; mp 208.0−210.0 °C; IR (KBr) υ = 3290, 3071, 2821, 2583, 2231, 1909, 2670, 1513, 1471, 1346, 1303, 1279, 1248, 1118, 1019, 968, 816, 799, 724, 668, 655 cm^{-1}; ^1H NMR (400 MHz, DMSO-d_6) δ 3.89 (s, 2H, CH_2), 4.02 (s, 2H, CH_2), 7.83 (dd, J = 9.0, 4.0 Hz, 1H, Ar-*H*), 8.59 (s, 1H, Ar-*H*), 8.96 (dd, J = 4.0, 1.5 Hz, 1H, Ar-*H*), 9.09 (dd, J = 9.0, 1.5 Hz, 1H, Ar-*H*); ^{13}C NMR (100 MHz, DMSO-d_6) δ 38.4, 50.9, 116.1, 118.9, 121.5, 125.0, 129.7, 132.6, 133.9, 136.8, 148.7, 158.6; HRMS (ESI) m/z calculated for $C_{12}H_{11}N_4O_3$ $[M + H]^+$ 259.0831, found 259.0834. Anal. ($C_{12}H_{10}N_4O_3$) C, H, N.

*6.9.2. Procedure for the Synthesis of 8-Cyanomethoxyquinoline (**26**).* To a solution of 8-hydroxyquinoline (**22**) (3.00 g, 20.69 mmol) and Cs_2CO_3 (13.50 g, 41.44 mmol) in DMSO (10 mL), bromoacetonitrile (1.30 g, 10.42 mmol, 0.8 mL) was added. The mixture was stirred at room temperature. After 30 min, another portion of bromoacetonitrile (1.30 g, 10.42 mmol, 0.8 mL) was added. The reaction was complete after stirring for an additional 30 min. Water (50 mL) was subsequently added and the product extracted with EtOAc (3× 80 mL). The combined organic phases were dried with Na_2SO_4, filtered, and removed under reduced pressure. The crude product was purified by column chromatography (EtOAc/hexane, 1/1) to yield 3.45 g (90%); pale yellow crystals; mp 118.5−120.5 °C; IR (KBr) υ = 3462, 2962, 2936, 2869, 2361, 1617, 1572, 1501, 1470, 1383, 1314, 1268, 1111, 820, 793, 751 cm^{-1}; ^1H NMR (500 MHz, $CDCl_3$) δ 5.19 (s, 2H, OCH_2), 7.31 (dd, J = 7.5, 1.0 Hz, 1H, Ar-*H*), 7.47−7.54 (m, 2H, Ar-*H*), 7.59 (dd, J = 8.5, 1.0 Hz, 1H, Ar-*H*), 8.19 (dd, J = 8.5, 1.5 Hz, 1H, Ar-*H*), 8.95 (dd, J = 4.0, 1.5 Hz, 1H, Ar-*H*); ^{13}C NMR (126 MHz, $CDCl_3$) δ 55.0, 112.5, 115.1, 122.1, 123.1, 126.4, 129.8, 136.3, 140.4, 149.9, 152.0; HRMS (ESI) m/z calculated for $C_{11}H_9N_2O$ $[M + H]^+$ 185.0715, found 185.0717. Anal. ($C_{11}H_8N_2O$) C, H, N.

*6.9.3. Procedure for the Synthesis of Compounds **27** and **28**.* To a cooled (0 °C) solution of KNO_3 (2.75 g, 27.20 mmol) in 97% H_2SO_4 (4 mL, 74.7 mmol), compound **26** (1.00 g, 5.44 mmol) was slowly added. The reaction mixture was initially stirred for 15 min at 0 °C and then for 1 h at room temperature. After the reaction was complete, the mixture was rapidly poured into a cold, saturated, aqueous solution of K_2CO_3. The precipitate that was formed was filtered off and washed with water, and the products **27** and **28** were separated and purified by column chromatography (CH_2Cl_2/MeOH, 20/1).

*8-Cyanomethoxy-5-nitroquinoline (**27**).* Yield, 85% (1.06 g); yellow crystals; mp 194.0−197.0 °C; IR (KBr) υ = 3443, 3098, 2951, 2889, 2361, 1618, 1563, 1505, 1464, 1395, 1327, 1301, 1242, 1177, 1102, 995, 796, 741, 710 cm^{-1}; ^1H NMR (500 MHz, DMSO-d_6) δ 5.58 (s, 2H, OCH_2), 7.52 (d, J = 9.0 Hz, 1H, Ar-*H*), 7.89 (dd, J = 9.0, 4.0 Hz, 1H, Ar-*H*), 8.62 (d, J = 9.0 Hz, 1H, Ar-*H*), 9.01 (dd, J = 9.0, 1.5 Hz, 1H, Ar-*H*), 9.06 (dd, J = 4.0, 1.5 Hz, 1H, Ar-*H*); ^{13}C NMR (126 MHz, DMSO-d_6) δ 54.7, 108.4, 116.0, 122.0, 125.1, 126.9, 131.9, 138.2, 138.9, 150.8, 157.0; HRMS (ESI) m/z calculated for $C_{11}H_8N_3O_3$ $[M + H]^+$ 230.0566, found 230.0555. Anal. ($C_{11}H_7N_3O_3$) C, H, N.

*8-Acetamidoxy-5-nitroquinoline (**28**).* Yield, 14% (174 mg); pale yellow crystals; mp 227.0−231.0 °C; IR (KBr) υ = 3533, 2458, 2362, 1683, 1617, 1566, 1507, 1395, 1336, 1310, 1259, 1101, 1005, 818, 745, 593 cm^{-1}; ^1H NMR (500 MHz, DMSO-d_6) δ 4.87 (s, 2H, OCH_2), 7.24 (d, J = 9.0 Hz, 1H, Ar-*H*), 7.55 (br d, 2H, NH_2), 7.86 (dd, J = 9.0, 4.0 Hz, 1H, Ar-*H*), 8.55 (d, J = 9.0 Hz, 1H, Ar-*H*), 9.01−9.04 (m, 2H, Ar-*H*); ^{13}C NMR (126 MHz, DMSO-d_6) δ 68.2, 108.5, 122.6, 125.4, 128.0, 132.3, 138.1, 139.2, 150.8, 159.7, 169.3; HRMS (ESI) m/z calculated for $C_{11}H_{10}N_3O_4$ $[M + H]^+$ 248.0671, found 248.0673. Anal. ($C_{11}H_9N_3O_4$) C, H, N.

*6.9.4. General Procedure for Microwave-Assisted Synthesis of 5-Nitro-8-quinolinylamines **38**−**48**.*[37] A mixture of compound **27** (115 mg, 0.50 mmol), the desired amine (1.5 mmol), and CH_3CN (2 mL) was irradiated in the focused microwave equipment at 100 °C (80 or 150 W) for the indicated time (15 min to 2 h). After the reaction was complete, the volatiles were removed under reduced pressure and the residue was purified by silica gel radial chromatography.

*8-(4-Methylpiperidin-1-yl)-5-nitroquinoline (**42**).* The reaction mixture was irradiated for 2 h at 150 W. Eluent for chromatography: CH_2Cl_2/MeOH, 25/1. Yield, 118 mg (87%); brown oil; IR (NaCl plates) υ = 2948, 2922, 1555, 1504, 1492, 1387, 1296, 1280, 1245, 1228, 1191, 1141, 1080, 971, 952, 814, 785, 741 cm^{-1}; ^1H NMR (500 MHz, DMSO-d_6) δ 0.99 (d, J = 6.5 Hz, 3H, CH_3), 1.41 (ddd, J = 16.0, 13.0, 3.5 Hz, 2H, piperidine-*H*), 1.65−1.74 (m, 1H, piperidine-*H*), 1.77 (dd, J = 13.0, 3.5 Hz, 2H, piperidine-*H*), 3.07−3.12 (m, 2H, piperidine-*H*), 4.35 (d, J = 13.0 Hz, 2H, piperidine-*H*), 7.15 (d, J = 9.5 Hz, 1H, Ar-*H*), 7.76 (dd, J = 9.0, 4.0 Hz, 1H, Ar-*H*), 8.44 (d, J = 9.0 Hz, 1H, Ar-*H*), 8.90 (dd, J = 4.0, 1.5 Hz, 1H, Ar-*H*), 9.15 (dd, J = 9.0, 1.5 Hz, 1H, Ar-*H*); ^{13}C NMR (126 MHz, DMSO-d_6) δ 21.8, 30.4, 33.9, 51.6, 112.0, 123.3, 124.3, 128.1, 132.1, 134.4, 139.5, 147.4, 155.1; HRMS (ESI) m/z calculated for $C_{15}H_{18}N_3O_2$ $[M + H]^+$ 272.1394, found 272.1387; purity by HPLC, 96.23%.

*6.9.5. Procedure for the Synthesis of 4-Nitronaphthalen-1-yl Methanesulfonate (**51**).* To a solution of 4-nitro-1-naphthol (**49**) (500 mg, 2.65 mmol) in CH_2Cl_2 (20 mL), methanesulfonyl chloride (600 mg, 0.53 mmol) and dry Et_3N (540 mg, 0.53 mmol, 0.73 mL) were added under argon. The reaction mixture was stirred at room temperature for 1 h. After the completion of the reaction, the mixture was extracted with 1 M HCl (2× 50 mL) and water (1× 50 mL), dried with Na_2SO_4, and filtered, and the solvent was removed under reduced pressure to yield 680 mg (97%) of dark yellow crystals that were used in the next step without further purification. ^1H NMR (500 MHz, DMSO-d_6) δ 2.24 (s, 3H, OSO_2CH_3), 7.63 (d, J = 8.5 Hz, 1H, Ar-*H*), 7.75 (ddd, J = 8.5, 7.0, 1.0 Hz, 1H, Ar-*H*), 7.82 (ddd, J = 8.5, 7.0, 1.0 Hz, 1H, Ar-*H*), 8.26−8.28 (m, 2H, Ar-*H*), 8.62 (dd, J = 8.5, 1.0 Hz, 1H, Ar-*H*).

*6.9.6. Procedure for the Synthesis of 4-Nitronaphthalene-1-pyrrolidine **52**.* The mixture of compound **51** (100 mg, 0.38 mmol) and pyrrolidine (133 mg, 1.87 mmol) in EtOH (2 mL) was irradiated in the focused microwave equipment at 100 °C (80 W) for 20 min. Following this, the volatiles were removed under reduced pressure, and the residue was purified by silica gel radial chromatography (EtOAc/hexane, 1/5) to yield 6 mg (7%); orange crystals; mp 123.0−125.0 °C; IR (KBr) υ = 3424, 2921, 2854, 2432, 1847, 1578, 1560, 1528, 1480, 1431, 1412, 1306, 1273, 1250, 1149, 1132, 946, 897, 758, 732 cm^{-1}; ^1H NMR (500 MHz, $CDCl_3$) δ 2.05−2.07 (m, 4H, pyrrolidine-*H*), 3.69−3.71 (m, 4H, pyrrolidine-*H*), 6.63 (d, J = 9.0 Hz, 1H, Ar-*H*), 7.43 (ddd, J = 8.5, 7.0, 1.0 Hz, 1H, Ar-*H*), 7.65 (ddd, J = 8.5, 7.0, 1.0 Hz, 1H, Ar-*H*), 8.24 (d, J = 9.0 Hz, 1H, Ar-*H*), 8.40 (dd, J = 8.5, 1.0 Hz, 1H, Ar-*H*), 8.97 (dd, J = 8.5, 1.0 Hz, 1H, Ar-*H*); ^{13}C NMR (126 MHz, $CDCl_3$) δ 26.0, 29.7, 53.2, 105.6, 124.0, 124.7, 125.9, 128.4, 128.8, 129.3, 135.7, 154.0; HRMS (ESI) m/z calculated for $C_{14}H_{15}N_2O_2$ $[M + H]^+$ 243.1128, found 243.1123. Anal. ($C_{14}H_{14}N_2O_2$) C, H, N.

*6.9.7. Procedure for the Synthesis of 2-Bromo-4-nitro-1-aminonaphthalene (**54**).* To a solution of BrCN (97%, 65.5 mg, 0.6 mmol) in dry THF (5 mL), a solution of compound **50** (188 mg, 1.0 mmol) in dry THF (3 mL) was slowly added under argon. After 24 h of stirring at room temperature, additional amounts of BrCN (211 mg, 2.0 mmol) were added. The reaction mixture was stirred at 60 °C until the starting material disappeared (24 h, monitored by TLC). The solvent was evaporated and the crude product purified by column chromatography (EtOAc/hexane, 1/1) to yield 137 mg (52%) of yellow solid; mp 246.0−248.0 °C (lit.[52] 250 °C); IR (KBr) υ = 3472, 3368, 3229, 2921, 1810, 1618, 1561, 1513, 1482, 1441, 1403, 1349, 1274, 1157, 1041, 992, 905, 835, 760, 686, 561 cm^{-1}; ^1H NMR (400 MHz, DMSO-d_6) δ 7.51 (br s, 2H, NH_2), 7.61 (ddd, J = 8.5, 7.0, 1.0 Hz, 1H, Ar-*H*), 7.79 (ddd, J = 9.0, 7.0, 1.0 Hz, 1H, Ar-*H*), 8.47 (dd, J = 8.5, 1.0 Hz, 1H, Ar-*H*), 8.56 (s, 1H, Ar-H), 8.80 (dd, J = 9.0, 1.0 Hz, 1H, Ar-*H*); ^{13}C NMR (100 MHz, DMSO-d_6) δ 97.5, 120.9, 123.5,

dx.doi.org/10.1021/jm301544x | J. Med. Chem. 2013, 56, 521−533

123.7, 126.2, 126.2, 130.3, 131.9, 132.6, 149.5; HRMS (ESI) m/z calcd for $C_{10}H_8BrN_2O_2$ $[M + H]^+$ 266.9769, found 266.9773. Anal. ($C_{10}H_7BrN_2O_2$) C, H, N.

■ ASSOCIATED CONTENT

Ⓢ Supporting Information

Figures, additional experimental details, and spectroscopic and analytical data for the intermediates and final compounds. This material is available free of charge via the Internet at http://pubs.acs.org.

■ AUTHOR INFORMATION

Corresponding Author

*Phone: +386-1-476-9500. Fax: +386-1-425-8031. E-mail: stanislav.gobec@ffa.uni-lj.si.

Author Contributions

⊥These authors contributed equally to this study.

Notes

The authors declare no competing financial interest.

■ ACKNOWLEDGMENTS

This work was supported by the Slovenian Research Agency. We thank Dr. Samo Turk for helping us with the docking experiments. We also thank OpenEye Scientific Software, Inc. for free academic licenses of their software.We also thank Dr. Chris Berrie for critical reading of the manuscript.

■ ABBREVIATIONS USED

Abz, 2-aminobenzoyl; AMC, 7-amido-4-methylcoumarin; catB, cathepsin B; catH, cathepsin H; catL, cathepsin L; DMSO, dimethyl sulfoxide; ECM, extracellular matrix; TMHI, 1,1,1-trimethylhydrazinium iodide; K_i, inhibition constant; Z, benzyloxycarbonyl

■ REFERENCES

(1) Rawlings, N. D.; Barrett, A. J.; Bateman, A. MEROPS: The Database of Proteolytic Enzymes, Their Substrates and Inhibitors. *Nucleic Acids Res.* **2012**, *40*, 343−350.

(2) Barrett, A. J.; Kirschke, H. Cathepsin B, Cathepsin H, and Cathepsin L. *Methods Enzymol.* **1981**, *80*, 535−561.

(3) Hill, P. A.; Docherty, A. J.; Bottomley, K. M.; O'Connell, J. P.; Morphy, J. R.; Reynolds, J. J.; Meikle, M. C. Inhibition of Bone Resorption in Vitro by Selective Inhibitors of Gelatinase and Collagenase. *Biochem. J.* **1995**, *308*, 167−175.

(4) Jordans, S.; Jenko-Kokalj, S.; Kühl, N. M.; Tedelind, S.; Sendt, W.; Brömme, D.; Turk, D.; Brix, K. Monitoring Compartment-Specific Substrate Cleavage by Cathepsins B, K, L, and S at Physiological pH and Redox Conditions. *BMC Biochem.* **2009**, *10*, 23.

(5) Zhang, T.; Maekawa, Y.; Hanba, J.; Dainichi, T.; Nashed, B. F.; Hisaeda, H.; Sakai, T.; Asao, T.; Himeno, K.; Good, R. A.; Katunuma, N. Lysosomal Cathepsin B Plays an Important Role in Antigen Processing, While Cathepsin D Is Involved in Degradation of the Invariant Chain in Ovalbumin-Immunized Mice. *Immunology* **2000**, *100*, 13−20.

(6) Hook, V.; Toneff, T.; Bogyo, M.; Greenbaum, D.; Medzihradszky, K. F.; Neveu, J.; Lane, W.; Hook, G.; Reisine, T. Inhibition of Cathepsin B Reduces Beta-Amyloid Production in Regulated Secretory Vesicles of Neuronal Chromaffin Cells: Evidence for Cathepsin B as a Candidate Beta-Secretase of Alzheimer's Disease. *Biol. Chem.* **2005**, *386*, 931−940.

(7) Hashimoto, Y.; Kakegawa, H.; Narita, Y.; Hachiya, Y.; Hayakawa, T.; Kos, J.; Turk, V.; Katunuma, N. Significance of Cathepsin B Accumulation in Synovial Fluid of Rheumatoid Arthritis. *Biochem. Biophys. Res. Commun.* **2001**, *283*, 334−339.

(8) Baici, A.; Lang, A.; Zwicky, R.; Müntener, K. Cathepsin B in Osteoarthritis: Uncontrolled Proteolysis in the Wrong Place. *Semin. Arthritis Rheum.* **2005**, *34*, 24−28.

(9) Van Acker, G. J. D.; Saluja, A. K.; Bhagat, L.; Singh, V. P.; Song, A. M.; Steer, M. L. Cathepsin B Inhibition Prevents Trypsinogen Activation and Reduces Pancreatitis Severity. *Am. J. Physiol.: Gastrointest. Liver Physiol.* **2002**, *283*, 794−800.

(10) Mohamed, M. M.; Sloane, B. F. Cysteine Cathepsins: Multifunctional Enzymes in Cancer. *Nat. Rev. Cancer* **2006**, *6*, 764−775.

(11) Kos, J.; Lah, T. T. Cysteine Proteinases and Their Endogenous Inhibitors: Target Proteins for Prognosis, Diagnosis and Therapy in Cancer. *Oncol. Rep.* **1998**, *5*, 1349−1361.

(12) Berdowska, I. Cysteine Proteases as Disease Markers. *Clin. Chim. Acta* **2004**, *342*, 41−69.

(13) Sloane, B.; Moin, K.; Sameni, M.; Tait, L.; Rozhin, J.; Ziegler, G. Membrane Association of Cathepsin B Can Be Induced by Transfection of Human Breast Epithelial Cells with c-Ha-ras Oncogene. *J. Cell Sci.* **1994**, *107*, 373−384.

(14) Linebaugh, B. E.; Sameni, M.; Day, N. A.; Sloane, B. F.; Keppler, D. Exocytosis of Active Cathepsin B. Enzyme Activity at pH 7.0, Inhibition and Molecular Mass. *Eur. J. Biochem.* **1999**, *264*, 100−109.

(15) Roshy, S.; Sloane, B. F.; Moin, K. Pericellular Cathepsin B and Malignant Progression. *Cancer Metastasis Rev.* **2003**, *22*, 271−286.

(16) Koblinski, J. E.; Ahram, M.; Sloane, B. F. Unraveling the Role of Proteases in Cancer. *Clin. Chim. Acta* **2000**, *291*, 113−135.

(17) Buck, M. R.; Karustis, D. G.; Day, N. A.; Honn, K. V.; Sloane, B. F. Degradation of Extracellular-Matrix Proteins by Human Cathepsin B from Normal and Tumour Tissues. *Biochem. J.* **1992**, *282*, 273−278.

(18) Premzl, A.; Zavašnik-Bergant, V.; Turk, V.; Kos, J. Intracellular and Extracellular Cathepsin B Facilitate Invasion of MCF-10A neoT Cells through Reconstituted Extracellular Matrix in Vitro. *Exp. Cell Res.* **2003**, *283*, 206−214.

(19) Mirković, B.; Premzl, A.; Hodnik, V.; Doljak, B.; Jevnikar, Z.; Anderluh, G.; Kos, J. Regulation of Cathepsin B Activity by 2A2 Monoclonal Antibody. *FEBS J.* **2009**, *276*, 4739−4751.

(20) Skrzydlewska, E.; Sulkowska, M.; Koda, M.; Sulkowski, S. Proteolytic−Antiproteolytic Balance and Its Regulation in Carcinogenesis. *World J. Gastroenterol.* **2005**, *11*, 1251−1266.

(21) Illy, C.; Quraishi, O.; Wang, J.; Purisima, E.; Vernet, T.; Mort, J. S. Role of the Occluding Loop in Cathepsin B Activity. *J. Biol. Chem.* **1997**, *272*, 1197−1202.

(22) Nägler, D. K.; Storer, A. C.; Portaro, F. C. V.; Carmona, E.; Juliano, L.; Ménard, R. Major Increase in Endopeptidase Activity of Human Cathepsin B upon Removal of Occluding Loop Contacts. *Biochemistry* **1997**, *36*, 12608−12615.

(23) Musil, D.; Zucic, D.; Turk, D.; Engh, R. A.; Mayr, I.; Huber, R.; Popovic, T.; Turk, V.; Towatari, T.; Katunuma, N.; Bode, W. The Refined 2.15 Å X-ray Crystal Structure of Human Liver Cathepsin B: The Structural Basis for Its Specificity. *EMBO J.* **1991**, *10*, 2321−2330.

(24) Almeida, P. C.; Nantes, I. L.; Chagas, J. R.; Rizzi, C. C.; Faljoni-Alario, A.; Carmona, E.; Juliano, L.; Nader, H. B.; Tersariol, I. L. Cathepsin B Activity Regulation. Heparin-like Glycosaminogylcans Protect Human Cathepsin B from Alkaline pH-Induced Inactivation. *J. Biol. Chem.* **2001**, *276*, 944−951.

(25) Pavlova, A.; Krupa, J. C.; Mort, J. S.; Abrahamson, M.; Björk, I. Cystatin Inhibition of Cathepsin B Requires Dislocation of the Proteinase Occluding Loop. Demonstration by Release of Loop Anchoring through Mutation of His110. *FEBS Lett.* **2000**, *487*, 156−160.

(26) Renko, M.; Požgan, U.; Majera, D.; Turk, D.; Stefin, A. Displaces the Occluding Loop of Cathepsin B Only by as Much as Required To Bind to the Active Site Cleft. *FEBS J.* **2010**, *277*, 4338−4345.

(27) Redzynia, I.; Ljunggren, A.; Abrahamson, M.; Mort, J. S.; Krupa, J. C.; Jaskolski, M.; Bujacz, G. Displacement of the Occluding Loop by the Parasite Protein, Chagasin, Results in Efficient Inhibition of Human Cathepsin B. *J. Biol. Chem.* **2008**, *283*, 22815−22825.

(28) Frlan, R.; Gobec, S. Inhibitors of Cathepsin B. *Curr. Med. Chem.* **2006**, *13*, 2309−2327.
(29) Turk, B. Targeting Proteases: Successes, Failures and Future Prospects. *Nat. Rev. Drug Discovery* **2006**, *5*, 785−799.
(30) Frizler, M.; Stirnberg, M.; Sisay, M. T.; Gütschow, M. Development of Nitrile-Based Peptidic Inhibitors of Cysteine Cathepsins. *Curr. Top. Med. Chem.* **2010**, *10*, 294−322.
(31) Mirković, B.; Renko, M.; Turk, S.; Sosič, I.; Jevnikar, Z.; Obermajer, N.; Turk, D.; Gobec, S.; Kos, J. Novel Mechanism of Cathepsin B Inhibition by Antibiotic Nitroxoline and Related Compounds. *ChemMedChem* **2011**, *6*, 1351−1356.
(32) Yamamoto, A.; Hara, T.; Tomoo, K.; Ishida, T.; Fujii, T.; Hata, Y.; Murata, M.; Kitamura, K. Binding Mode of CA074, a Specific Irreversible Inhibitor, to Bovine Cathepsin B As Determined by X-ray Crystal Analysis of the Complex. *J. Biochem.* **1997**, *121*, 974−979.
(33) Towatari, T.; Nikawa, T.; Murata, M.; Yokoo, C.; Tamai, M.; Hanada, K.; Katunuma, N. Novel Epoxysuccinyl Peptides. A Selective Inhibitor of Cathepsin B, in Vivo. *FEBS Lett.* **1991**, *280*, 311−315.
(34) Meanwell, N. A. Synopsis of Some Recent Tactical Application of Bioisosteres in Drug Design. *J. Med. Chem.* **2011**, *54*, 2529−2591.
(35) M Movrin, D.; Maysinger, E. M. Biologically Active Mannich Bases Derived from Nitroxoline. *Pharmazie* **1980**, *35*, 458−460.
(36) Grzegozek, M. Vicarious Nucleophilic Amination of Nitroquinolines by 1,1,1-Trimethylhydrazinium Iodide. *J. Heterocycl. Chem.* **2008**, *45*, 1879−1882.
(37) Štefane, B.; Požgan, F.; Sosič, I.; Gobec, S. A Microwave-Assisted Nucleophilic Substitution Reaction on a Quinoline System: The Synthesis of Amino Analogues of Nitroxoline. *Tetrahedron Lett.* **2012**, *53*, 1964−1967.
(38) Mirković, B.; Sosič, I.; Gobec, S.; Kos, J. Redox-Based Inactivation of Cysteine Cathepsins by Compounds Containing the 4-Aminophenol Moiety. *PLoS One* **2011**, *6*, e27197.
(39) Watanabe, D.; Yamamoto, A.; Tomoo, K.; Matsumoto, K.; Murata, M.; Kitamura, K.; Ishida, T. Quantitative Evaluation of Each Catalytic Subsite of Cathepsin B for Inhibitory Activity Based on Inhibitory Activity-Binding Mode Relationship of Epoxysuccinyl Inhibitors by X-ray Crystal Structure Analyses of Complexes. *J. Mol. Biol.* **2006**, *362*, 979−993.
(40) Tomoo, K. Development of Cathepsin Inhibitors and Structure-Based Design of Cathepsin B-Specific Inhibitor. *Curr. Top. Med. Chem.* **2010**, *10*, 696−707.
(41) Cathers, B. E.; Barrett, C.; Palmer, J. T.; Rydzewski, R. M. pH Dependence of Inhibitors Targeting the Occluding Loop of Cathepsin B. *Bioorg. Chem.* **2002**, *30*, 264−275.
(42) Sorokin, L. The Impact of the Extracellular Matrix on Inflammation. *Nat. Rev. Immunol.* **2010**, *10*, 712−723.
(43) Szpaderska, A. M.; Frankfater, A. An Intracellular Form of Cathepsin B Contributes to Invasiveness in Cancer. *Cancer Res.* **2001**, *61*, 3493−3500.
(44) Premzl, A.; Turk, V.; Kos, J. Intracellular Proteolytic Activity of Cathepsin B Is Associated with Capillary-like Tube Formation by Endothelial Cells in Vitro. *J. Cell. Biochem.* **2006**, *97*, 1230−1240.
(45) Sevenich, L.; Schurigt, U.; Sachse, K.; Gajda, M.; Werner, F.; Müller, S.; Vasiljeva, O.; Schwinde, A.; Klemm, N.; Deussing, J.; Peters, C.; Reinheckel, T. Synergistic Antitumor Effects of Combined Cathepsin B and Cathepsin Z Deficiencies on Breast Cancer Progression and Metastasis in Mice. *Proc. Natl. Acad. Sci. U.S.A.* **2010**, *107*, 2497−2502.
(46) Perola, E. An Analysis of the Binding Effinciencies of Drugs and Their Leads in Successful Drug Discovery Programs. *J. Med. Chem.* **2010**, *53*, 2986−2997.
(47) Kuhelj, R.; Dolinar, M.; Pungercar, J.; Turk, V. The Preparation of Catalytically Active Human Cathepsin B from Its Precursor Expressed in *Escherichia coli* in the Form of Inclusion Bodies. *Eur. J. Biochem.* **1995**, *229*, 533−539.
(48) Schweiger, A.; Štabuc, B.; Popović, T.; Turk, V.; Kos, J. Enzyme-Linked Immunosorbent Assay for the Detection of Total Cathepsin H in Human Tissue Cytosols and Sera. *J. Immunol. Methods* **1997**, *201*, 165−172.
(49) Dolinar, M.; Maganja, D. B.; Turk, V. Expression of Full-Length Human Procathepsin L cDNA in *Escherichia coli* and Refolding of the Expression Product. *Biol. Chem. Hoppe-Seyler* **1995**, *376*, 385−388.
(50) Feng, B. Y.; Shoichet, B. K. A Detergent-Based Assay for the Detection of Promiscuous Inhibitors. *Nat. Protoc.* **2006**, *1*, 550−553.
(51) Eisenberg, M. C.; Kim, Y.; Li, R.; Ackerman, W. E.; Kniss, D. A.; Friedman, A. Mechanistic Modeling of the Effects of Myoferlin on Tumor Cell Invasion. *Proc. Natl. Acad. Sci. U.S.A.* **2011**, *108*, 20078−20083.
(52) Hodgson, H. H.; Elliott, R. L. 373. The 3-Halogeno-1-nitro-, -1-amino-, and -1-hydroxy-naphthalenes. *J. Chem. Soc.* **1934**, 1705.